

Novel Ru(II) Heteroleptic Complexes Anchored to TiO₂ Nanocrystalline: Synthesis, Characterization and Application to Dye-sensitized Solar Cells

Hashem Shahroosvand* and Fahimeh Nasouti

Chemistry Department, University of Zanjan, Zanjan, Iran

Received: March 28, 2012, Accepted: July 03, 2012, Available online: August 15, 2012

Abstract: A series of heteroleptic ruthenium(II) complexes from Ru(NO)(NO₃)₃ as precursor have been designed, synthesized and characterized by ¹H-NMR, FT-IR, UV-Vis, PL, ICP and CHN analyses. The reaction details and features were described in detail. Solar cells involving thin films of anatase TiO₂ impregnated with these dyes were prepared using an electrolyte solution of I/I₃⁻ in acetonitrile as the electron mediator, and their photovoltaic performance was evaluated. The system lacking carboxyl moiety as anchoring groups shows poor photovoltaic performance. We found that the efficiency of cell is strongly affected by the presence of carboxyl groups of the sensitizing dye, the efficiency of 1,2,4,5-benzenetetracarboxylic acid (btec) ruthenium(II) (with three btec moieties) adsorbed on TiO₂ nanocrystalline films being 4 times as large as that of bahtophenathroline ruthenium(II) (with one nitrate group) adsorbed on the same films. An incident photon-to-current conversion efficiency (IPCE) of 8% at 510 nm was obtained for tris(1,2,4,5-benzenetetracarboxylic acid) ruthenium(II) (4).

Keywords: Nanocrystalline; DSSC, Heteroleptic; Anchoring group.

1. INTRODUCTION

The development of systems for converting solar energy into electricity is among the most demanding challenges that scientists face today [1]. An important aspect of solar energy conversion involves the design and optimization of dye-sensitized solar cells (DSSCs). If properly optimized, DSSCs may function as low cost, efficient alternatives to conventional solid-state semiconductor devices [2]. In light harvesting, the first step in such conversion, the choice of a photosensitizer capable of efficient visible-light absorption is crucial. Therefore, many efforts have focused on the design and synthesis of various dyes, including metal complexes and organic dyes [3]. Understanding the relation between the solar cell performance and the properties of sensitizer molecule structures is one of the most important tasks for developing a high performance solar cell. Many molecular properties, such as the redox potential, the light harvesting efficiency, and the lifetime of the excited state, actually correlate with the solar cell performance [4]. Differences in the modes of binding of the dye to the semiconductor are likely to influence the electronic coupling between the dye and the semiconductor, thereby affecting the dynamics of both injection and recombination of the charge separated state of the

dye/TiO₂ moieties [5-8]. The development of molecular linkers to the surface is attracting increasing attention [9]. Rigid linkers varying in length and structure that have the shape of tripods were developed to study interfacial charge injection processes [10]. Ruthenium polypyridyl dyes have received much attention due to their outstanding performance as sensitizers in DSSC, reaching efficiencies of up to 11% [11-14]. Very recently, Michel Grätzel and et al were discovered a new porphyrin-sensitized solar cells with cobalt(II/III)-based redox electrolyte exceed 12 percent efficiency [15]. Recently, we reported the effect of the anchoring groups on the solar cell performance of Ru complexes using phen-dione ligands as sensitizer [16]. Here, we have investigated the binding of dyes to nanocrystalline TiO₂ as a function of the anchoring groups and the type of auxiliary ligands on the metal complexes.

2. EXPERIMENTAL

2. 1. Materials and Methods

All chemicals and solvents were purchased from Merck & Aldrich and used without further purification. ¹H-NMR spectra were recorded by use of a Bruker 250 MHz, spectrometer. IR spectra were recorded on a Perkin-Elmer 597 spectrometer. The PL spectra of the ruthenium compounds were measured in DMF solution.

*To whom correspondence should be addressed: Email: shahroos@znu.ac.ir
Fax.: +982415152584

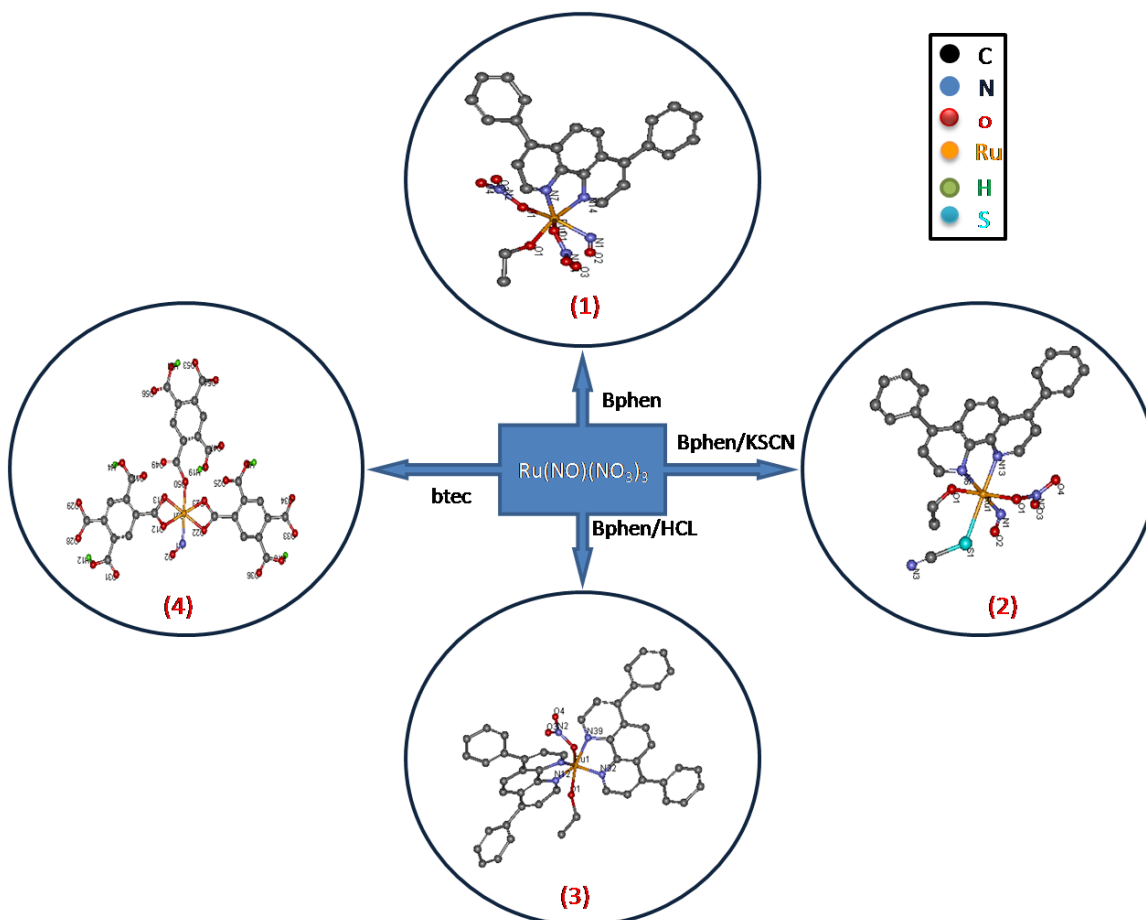


Figure 1. General procedure of synthesised ruthenium complexes in different conditions and molecular structure of the investigated ruthenium complexes.

The PL spectra were recorded by ocean optic spectrometer USB2000 during 325 nm irradiation. As a typical procedure, four new complexes of ruthenium nitrosyl with 1,2,4,5-benzenetetracarboxylic acid (btec acid), BPhenanthroline (BPhen) and tetra ammonium hexafluoride phosphate were synthesized by changes in the type of reactants as shown in Fig. 1.

Within 30 min a dark-brown precipitate was formed, and the mixture was allowed to reflux for 2 hours, cooled down, and filtered. It was washed with several portions of ethanol.

For the complex (3), Ru solution was refluxed with HCL, then the BPhen ligand was added to result. The Fabrication of TiO_2 Nanocrystalline electrodes, counter Pt-electrodes and DSC assemblage have been reported in elsevier in detail [1,11].

2.2. Fabrication of TiO_2 Nanocrystalline electrodes

To prepare the DSC working electrodes, the TCO glass used as current collector was first cleaned in a detergent solution using an ultrasonic bath for 15 min, and then rinsed with water and ethanol. Then the TCO glass plates were immersed into a 40 mM aqueous TiCl_4 solution at 70 °C for 30 min and washed with water and ethanol. A layer of TiCl_4 was coated on the TCO glass plates by screen-printing, kept in a clean box for 3 min so that the layer can relax to reduce the surface irregularity and then dried for 6 min at 125 °C.

After drying the films at 125 °C, The mesoscopic TiO_2 film used as photoanodes consisted of layers of TiO_2 (three 13 μm thick transparent layer of 25 nm TiO_2 anatase nanoparticles and a 10 μm thick scattering layer of 400 nm anatase TiO_2 particles). The multi layer films were heated to 520 °C and sintered for 30 min, then cooled to ~ 80 °C and immersed into the dye solution at room temperature for 16 h.

2.3. Preparation of counter Pt-electrodes

To prepare the counter electrode, The TCO sheet was washed with H_2O as well as with a 0.1 M HCL solution in ethanol and cleaned by ultrasound in an acetone bath for 10 min. After removing residual organic contaminants by heating in air for 15 min at 400 °C, the Pt catalyst was deposited on the TCO glass by coating with a drop of H_2PtCl_6 solution (2 mg Pt in 1 ml ethanol) with repetition of the heat treatment at 400 °C for 15 min.

2.4. DSC assemblage

The dye-covered TiO_2 electrode and Pt-counter electrode were assembled into a sandwich type cell. the two clips were Used to hold the two electrodes together at the corner of the plates. The electrolyte was injected into the space between two electrodes.

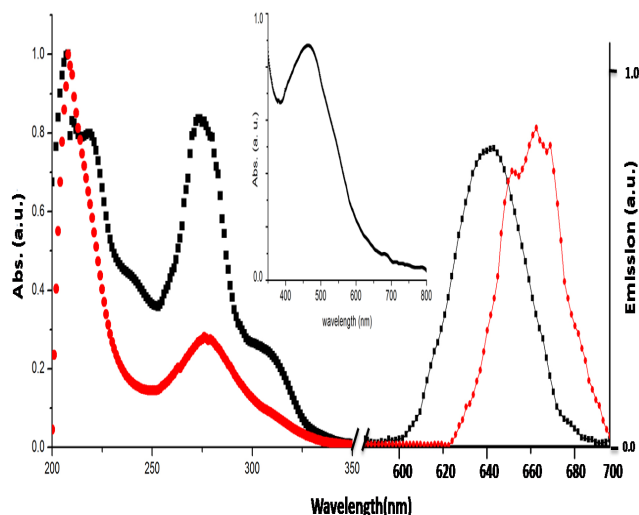


Figure 2. left: UV-vis spectra of complexes (1); black line and (4); red line in DMF solvent with 10⁻³ M concentration. Inset: Zoomed region of UV-vis spectrum of (4). right: PL spectra of complexes (1) and (4) in DMF solvent with 10⁻³ M concentration.

2.5. Photocurrent–voltage measurements

The irradiation source for the photocurrent–voltage (I–V) measurement is a 450 W xenon light source, which simulates the solar light. The current–voltage curves were obtained by measuring the photocurrent of the cells.

3. RESULTS AND DISCUSSION

3.1. Characterization of complexes

The wavelengths of maximum absorbance of the metal to ligand charge transfer (MLCT) $d \rightarrow \pi^*$ transition and maximum photoluminescence emission are shown in Table 1. Free H₄btec ligand shows three peaks at 213, 253 and 293 nm and BPhen shows peaks at 206, 221, 240, 274, 310 and 334 nm in UV-vis spectra. The changes of wavelength are found between the spectra of the complexes (1) and (4) that of the ligands, which confirms that the UV spectra of the complexes reflect an essentially absorption of the ligands. Also, broad band absorption in the regions of 450–600 nm is observed which are attributed to metal to ligand charge transition.

The luminescence property of synthesized complexes was investigated at room temperature. As shown in Fig. 2, Upon excitation at

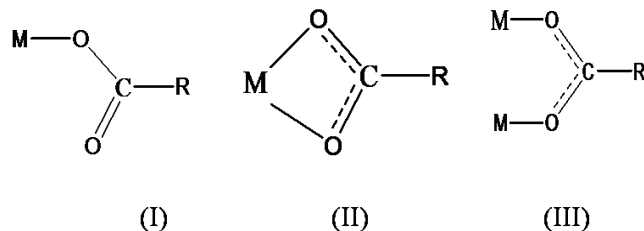


Figure 3. The possible mode of coordination of carboxylic acid.

exc = 340 nm, complex (4) emits a broad band at 640nm, while in complex (1) the corresponding peaks are red shifted and appear at 660 nm.

In order to understand the nature of the emission, we analyzed the photoluminescent properties of the free organic ligand and found that the strongest emission peak of btec acid is at 395 nm and 415 nm. It can be seen that the maximum emission peak of complexes (1) and (4) occur as a remarkable bathochromic shift. So this emission could be assigned to ligand-to-metal charge transfer (LMCT). The characterization of the binding is generally obtained by IR [17,18] and other methods [19]. The main absorption peaks in the IR spectra of the four complexes are determined. The difference in $\nu_{as}(\text{COO})$ and $\nu_s(\text{COO})$ ($\Delta\nu$), compared to the corresponding values in sodium carboxylate (95 cm⁻¹ in Na₄btec), is currently employed to determine the corresponding mode of the carboxylate group [20]. I. Unidentate complexes (structure I) exhibit the Δ values [$\nu_a(\text{CO}_2^-) - \nu_s(\text{CO}_2^-)$] which are much greater than the ionic values. II. Chelating (bidentate) complexes (structure II) exhibit Δ values which are significantly less than the ionic values. III. The Δ values for bridging complexes (structure III) are greater than those of chelating (bidentate) complexes, and close to the ionic values.

With considering above explanation, complexes (4) exhibit $\nu_{as}(\text{OCO})$ and $\nu_s(\text{OCO})$ vibrations of the carboxylate groups which occur at around 1623, 1541 and 1388, 1490, respectively. Therefore, monodentate mode (I) with $\Delta\nu = 235$ and bidentate mode (II) (51 cm⁻¹ < 95 cm⁻¹) were obtained (supporting informations). In general, the bonding between a d⁶ low-spin-metal center and NO is outstandingly strong, which assumes the M–NO⁺ structure. The Ru–NO frequency is appear at 1800–1950 cm⁻¹ which indicates that formally a linear NO⁺ is coordinated to the ruthenium(II) center [21]. The values of vibration of NO and NO₃ ligands are summarized in table 1.

Table 1, FT-IR (a: cm⁻¹), UV-vis (b: nm) data and PL data.

No.	IR						UV-Vis		PL
	$\nu_{as}(\text{COO})^a$	$\nu_s(\text{COO})^a$	$\Delta\nu^a$	$\nu(\text{NO})^a$	$\nu_s(\text{NO}_3)^a$	$\nu_{as}(\text{NO}_3)^a$	$\Pi \rightarrow \Pi^{*b}$	MLCT ^b	
1	-	-	-	1841	1383	1620	204, 221, 286, 310	510	670
2	-	-	-	1854	1384	1619	202, 222, 282, 312	528	655
3	-	-	-	-	1383	1555	205, 220, 275, 314	520	640
4	1623	1388	235	1893	-	-	218, 275	515	650
	1541	1490	51						

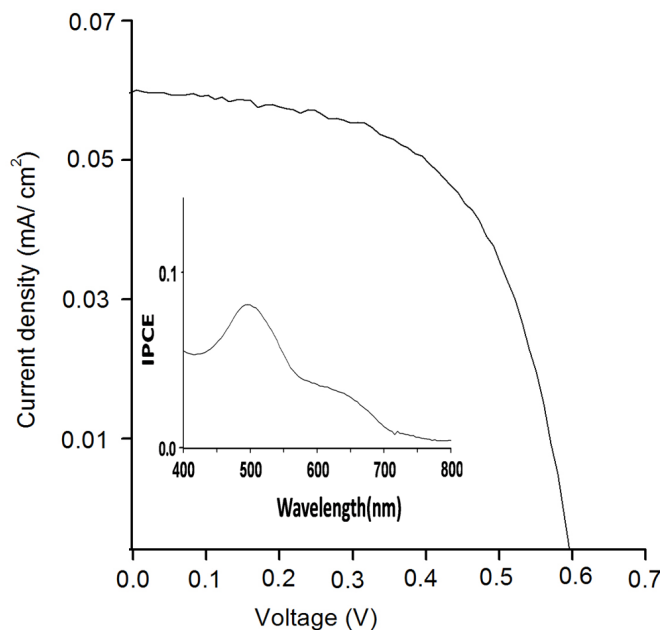


Figure 4. I-V curve of DSCs based on the complex (4) sensitizer. Inset: IPCE of complex (4).

CHN and ICP analysis were carried out to determine the presence of ligands and metal in the complexes. CHN analysis of compounds were obtained: Anal. Calc. for (1), $(C_{26}H_{21}N_5O_8Ru)$: C, 48.613; H, 3.143; N, 9.255. Found: C, 48.644; H, 3.128; N, 9.246%. Anal. Calc. for (2), $(C_{27}H_{21}N_5O_5SRu)$: C, 46.898; H, 2.989; N, 10.197. Found: C, 46.883; H, 2.979; N, 10.159%. Anal. Calc. for (3), $(C_{48}H_{37}N_5O_4Ru)$: C, 68.701; H, 4.097; N, 8.347. Found: C, 68.697; H, 4.034; N, 8.313%. Anal. Calc. for (4), $(C_{30}H_{14}NO_{25}Ru)$: C, 40.897; H, 0.994; N, 2.143. Found: C, 40.892; H, 0.987; N, 2.137%. Ru was analyzed on a PLASMA-SPEC (I) ICP atomic emission spectrometer. A few mg of complexes (0.02g) were destroyed in HNO_3 (68%) and finally diluted in water to 1:10 for being measured. The found concentrations for all complexes were estimated about 2.1-2.4 ppm. Further information on the complexes was obtained from 1H -NMR spectroscopy. 1H -NMR spectra for complex (4) shows one sharp peak at 7.50 ppm due to the btec acid. For other complexes, peaks at region 7.2 -8.5 ppm due to the Bphen that indicate the presence of ligands in complexes (supporting informations). The occurrence of only six Bphen signals for complex (3) and one btec signal for complex (4) confirm the presence of one compound, in which the two Bphen units for compound (4) and three btec for compound (3) have an identical chemical environments. The difference between the chemical shift of free ligands and complexes indicates that the coordination of ligands to metal is occurred. The signal integration for complexes (1, 2) reveals the incorporation of one Bphen unit. For complex (3), two Bphen unit were found by signal integration. Also, three btec units were revealed by signal integration for complexes (4). The sharp resonance indicates diamagnetic behavior of Ru(II) complexes with t_{2g}^6 configuration.

3.2. Photovoltaic Features

The photovoltaic performance of thin films of anatase TiO_2 impregnated with the dyes (1-4) was evaluated using an electrolyte solution of I^-/I_3^- in acetonitrile as the electron mediator.

The corresponding photoaction spectra are shown in Figure 4. In this series of Ru complexes, the highest incident monochromatic photon-to-current conversion efficiency (IPCE) was obtained for compound (4) (8% at 510 nm).

The value of IPCE could be interpreted in terms of better electronic coupling with the surface Ti^{4+} centers due to the fact that carboxyl group can be adsorbed deeper into the surface. IPCE values for other complexes (1-3) were below % 4 at 500 nm. From the data presented here, it can be concluded that even small changes in the structure resulting from the introduction of different functional groups (used for grafting) can considerably influence the efficiency of photoconversion. Furthermore, the binding of this type of inorganic sensitizer to the semiconductor surface, one critical factor in efficiency of solar cells. Typical current/voltage characteristics for photoelectrochemical cells sensitized with dye (4) is shown in Figure 4, with the corresponding device efficiencies given in table 2.

From table 2, it is apparent that (4) exhibits the highest photovoltaic device performance of the studied dye series. This device efficiency, however, remains low compared to the more established sensitizer dye, the ditetrabutylammonium salt of $[RuL_2(NCS)_2]$ (L) 2,2'-bipyridyl-4,4'-dicarboxylato, commonly called N719. This lower device efficiency can be primarily attributed to the relatively low optical absorbance of (4) compared to $[RuL_2(NCS)_2]$. It is useful to note, the efficiency of the our device based on N719 was obtained % 5.43.

The poor performances of the (1-3) based devices are reminiscent of the reported behavior of DSSCs based on $Ru(NCS)_2L_1L_2$, with $L_2 = NO_2^-$ or NH_2^- -substituted phenanthroline ligand [22].

To understand the reason behind the observation of different electron injection rates in TiO_2 -adsorbed compound (1) and compound (4) we used the Discovery Visualizer Studio to determine the geometric features of the deposited dye. We first built an infinite anatase crystal lattice and then locked the positions of all the O and Ti atoms in the anatase block. Dye molecules were deposited on the surface by creating ester bonds and nitrate bands between surface Ti atoms and carboxylic and nitrate O atoms. Figure 5 shows views of (1) and (4) on the anatase surfaces. In the dye (4), the geometry optimization led to a shortest O carboxylate-Ti surface distance of 18.43.5 Å.

In the dye (1), a shortest O nitrate-Ti surface distance is 10.13 Å. It seems that, the donor-acceptor distance is remarkably dependent upon the energy level of the anchoring groups. For the NO_3^- -substituted ligand, the poor performance has been discussed in terms of the unusually deep LUMO level coupled with the dominant LUMO population on ligand remote from the TiO_2 surface,

Table 2. I-V measurements of dyes (1-4).

NO.	J_{sc} (mA/cm ²)	V_{oc} (mV)	ff	η (%)
(1)	0.02	0.50	0.51	0.051
(2)	0.022	0.53	0.52	0.022
(3)	0.01	0.44	0.45	0.019
(4)	0.061	0.53	0.57	0.184

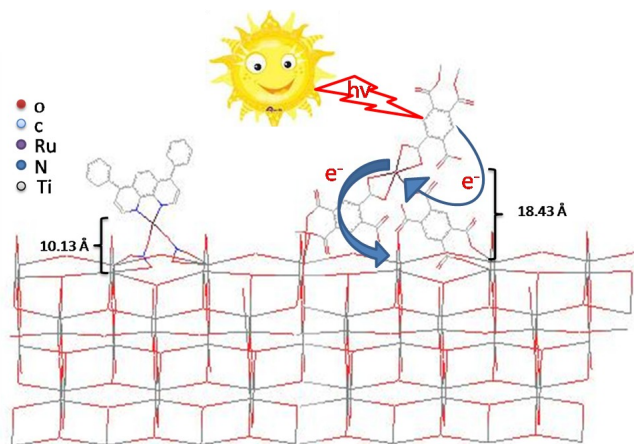


Figure 5. TiO₂-anatase nanostructures extended along the [101] directions sensitized by dye (1); left and (4); right. NO ligands are omitted for more clarity.

which cause inefficient electron injection from the excited-state dye into the TiO₂ conduction band [23].

4. CONCLUSION

Novel Ruthenium Heteroleptic Complexes have been synthesized by using ruthenium nitrosyl nitrat, either H₂btec or BPhen as photosensitizers for titanium dioxide semiconductor solar cells. The relative injection efficiency for derivatives of Ru complexes adsorbed on TiO₂ films and found that a molecule having nitrate as anchoring group exhibited a very low efficiency compared with a molecule having carboxyl groups. Incident photon-to-current conversion efficiency (IPCE) is sensitive to the structural changes that resulted from introducing different functional groups, used for grafting. Further work on ruthenium complexes with other polypyridin ligands is in progress, and we believe improvement can be accomplished by a thorough replacement of attached functionalized groups to ruthenium complexes in DSSC field.

REFERENCES

[1] (a) B. O'Regan, M. Gratzel, *Nature*, 353, 737 (1991). (b) M. Grätzel, *Inorg. Chem.*, 44, 6841 (2005).
 [2] A. Kukrek, D. Wang, Y. Hou, R. Zong, R. Thummel, *Inorg. Chem.*, 45, 10131 (2006).
 [3] W.S. Han, J.K. Han, H.Y. Kim, M.J. Choi, Y.S. Kang, C. Pac, S.O.Kang, *Inorg. Chem.*, 50, 3271 (2011),
 [4] K. Hara, H. Horiuchi, R. Katoh, L.P. Singh, H. Sugihara, K. Sayama, S. Murata, M. Tachiya, H. Arakawa, *J. Phys. Chem. B*, 106, 374 (2002).
 [5] A. Fillinger, B.A. Parkinson, *J. Electrochem. Soc.*, 146, 4559 (1999).
 [6] K. Murakoshi, G. Kano, Y. Wada, S Yanagida. H. Miyazaki, M. Matsumoto, S. Murasawa, *J. Electroanal. Chem.*, 396, 27 (1995).
 [7] K. Hara, H. Sugihara, L. P. Singh, A. Islam, R. Katoh, M. Yanagida, K. Sayama, S Murata, H. Arakawa, *J. Photochem.*

Photobiol., A, 145, 117 (2001),
 [8] (a) K. Kilså, E.I. Mayo, B.S. Brunschwig, H.B. Gray, N.S. Lewis, J.R. Winkler, *J. Phys. Chem. B*, 108, 15640 (2004). (b) A. Sepehrifard, A. Stublla, S. Haftchenary, S. Chen, P.G. Potvin, S. Morin, *J. New Mat. Electrochem. Systems*, 11, 281 (2008).
 [9] E. Galoppini, *Coord. Chem. Rev.*, 248, 1283 (2004).
 [10] D. Wang, R. Mendelsohn, E. Galoppini, *J. Phys. Chem. B*, 108, 16642 (2004).
 [11] M. K. Nazeeruddin, A. Kay, I. Rodicio, R. Humphry-Baker, E. Mueller, P. Liska, N. Vlachopoulos, M. Graetzel, *J. Am. Chem. Soc.*, 115, 6382 (1993).
 [12] C.A. Bignozzi, R. Argazzi, C. Kleverlaan, *J. Chem. Soc. Rev.*, 29, 87 (2000).
 [13] Nazeeruddin, M.K.; Graetzel, M. *Comp. Coord. Chem. II*, 9, 719 (2004).
 [14] E.A.M. Geary, L.J. Yellowlees, L.A. Jack, I.D.H. Oswald, S. Parsons, N. Hirata, J.R. Durrant, N. Robertson, *Inorg. Chem.*, 44, 242 (2005)
 [15] A. Yella, H.W. Lee, H.N. Tsao, C. Yi, A.K. Chandiran, M.K. Nazeeruddin, E.W. Guang Diao, C.Y. Yeh, S.M. Zakeeruddin, M. Grätzel, *Science*, 334, 629 (2011).
 [16] H. Shahroosvand, M. Khorasani-Motlagh, M. Noroozifar, M. Shabani, A. Fyezbaksh, M. Abdouss, *Int. J. Nanomanufacturing*, 5, 352 (2010). (b) H. Shahroosvand, P. Abbasi, M. Ameri, M. R. Riahi Dehkordi, *Int. J. Photoenergy*, 2011, 1 (2011).
 [17] R. Argazzi, C.A. Bignozzi, T.A. Heimer, F.N. Castellano, G.J. Meyer, *Inorg. Chem.*, 33, 5741(1994).
 [18] (a) A. Hugot-Le Goff, S. Joiret, P. Faralas, *J. Phys. Chem. B*, 103, 9569 (1999). (b) S. Umpathy, A.M. Cartner, A.W. Parker, R.E. Hester, *J. Phys. Chem.*, 94, 1357 (1990).
 [19] Y.-X. Weng, L. Li, Y. Liu, L. Wang, G.-Z. Yang, *J. Phys. Chem. B*, 107, 4356 (2003).
 [20] (a). R. Cao, Q. Shi, D. Sun, M. Hong, W. Bi, and Y. Zhao, *Inorg. Chem.*, 41, 6161 (2002). (b) Y. Hou, S. Wang, E. Shen, E. Wang, D. Xiao, Y. Li, L. Xu, C. Hu, *Inorg. Chim. Acta*, 357, 3155 (2004). (c) Z. Tian, T. Song, Y. Fan, S. Shi, L. Wang, *Inorg. Chim. Acta*, 360, 3424 (2007). (d) D. Cheng, M. A. Khan, R. P. Houser, *Inorg. Chim. Acta*, 351, 242 (2003).
 [21]. (a) H. J. Xu, Y. Cheng, J. F. Sun, B. A. Dougan, Y. Z. Li, X. T. Chen, Z. L. Xue, *J. Organomet. Chem.* 693, 3851 (2008). (b) M. J. Rose, P. K. Mascharak, *Coord. Chem. Rev.* 252, 2093 (2008). (c) G. V. Poelhsitz, A. L. Bogado, G. D. de Souza, E. R. Filho, A. A. Batista, M. P. de Araujo, *Inorg. Chem. Commun.*, 10, 133 (2007).
 [22] A. Reynal, A. Forneli, E. Martinez-Ferrero, A. Sanchez-Díaz, A. Vidal-Ferran, B. C O'Regan, E. Palomares. *J. Am. Chem. Soc.*, 130, 13558 (2008).
 [23] W.S. Han, J.K. Han, H.Y. Kim, M.J. Choi, Y.S. Kang, C. Pac, S.O. Kang, *Inorg. Chem.*, 50, 3271 (2011).